



ISSN 1349-1113
JAXA-RR-07-014E

JAXA Research and Development Report

**Thermophysical Properties of Liquid and
Supercooled Rare Earth Elements Measured by
an Electrostatic Levitator**

Takehiko ISHIKAWA, Paul-FRANÇOIS PARADIS,
Yuki WATANABE and Noriyuki KOIKE

February 2008

Japan Aerospace Exploration Agency

Thermophysical Properties of Liquid and Supercooled Rare Earth Elements Measured by an Electrostatic Levitator

By

Takehiko ISHIKAWA^{*1}, Paul-FRANÇOIS PARADIS^{*1},
Yuki WATANABE^{*2} and Noriyuki KOIKE^{*3}

Abstract: Thermophysical properties of four rare earth elements, namely lanthanum (La), praseodymium (Pr), neodymium (Nd), and terbium (Tb) have been measured using electrostatic levitation techniques. The understanding of the nature and behavior of rare earth metals in their liquid phases requires accurate values of their physical properties. However, keeping samples in their liquid phases free from contamination long enough to carry out measurements represents a formidable challenge. This is due to high reactivity and melts contamination of these elements with crucibles or gaseous environment. The use of an electrostatic levitator in vacuum conditions circumvents these difficulties and permits the measurements of the density, the surface tension, and the viscosity of these metals above and below their melting temperature. In this paper, the measurement methods as well as the levitation apparatus are introduced and measured values are reported.

Key words: rare earth elements, liquid, density, surface tension, viscosity

1. Introduction

Lanthanum, praseodymium, neodymium and their compounds are currently used to improve the resistance of certain glasses, to fabricate hydrogen sponges and strong magnets, and as dopants in optical amplifiers¹⁾. Terbium has found applications as a dopant in materials that are used in solid-state devices (e.g., photovoltaic cells, laser amplifiers) and as a stabilizer of fuel cells which operate at high temperatures. Terbium is also utilized in alloys and in the production of television tubes and fluorescent lamps¹⁾. To assist further material development, the knowledge of the physical properties of rare earth metals and their temperature dependences is therefore paramount. However, La, Pr, Nd, and Tb are very reactive, oxidizing rapidly when exposed to air and reacting directly with nitrogen and other elements¹⁾.

This explains why accurate physical properties are difficult to measure above their melting points when traditional methods are used (e.g., crucible, support) and why there are no data reported in the undercooled region. Here, electrostatic levitation in vacuum isolated a sample against contaminating walls and surrounding gases²⁻⁵⁾. This circumvented the problems related to high temperature processing and allowed an accurate non-contact determination of the density, the surface tension, and the viscosity of liquid La, Pr, Nd, and Tb. This paper shortly introduces the facility, describes the processing and property determination methods, and then presents preliminary experimental results.

*1 Japan Aerospace Exploration Agency, 2-1-1 Sengen, Tsukuba, Ibaraki, Japan 305-8505.

*2 Advanced Engineering Services Co. Ltd., 1-6-1 Takezono, Tsukuba, Ibaraki, Japan.

*3 Chiba Institute of Technology, 2-17-1 Tsudanuma, Narashino, Chiba, Japan.

2. Experimental Setup and Procedures

2.1. Electrostatic Levitation Furnace

The measurements were made using an electrostatic levitator (Fig. 1)²⁾ which consisted of a chamber evacuated to a $\sim 10^{-5}$ Pa vacuum level before processing was initiated. The chamber housed a sample charged by electronic emission and levitated between electrodes via a feedback loop. The two disk electrodes were used for the vertical position control whereas four spherical electrodes were dedicated to horizontal control⁶⁾. The positioning control relied on two sets of orthogonally arranged He-Ne lasers and the associated position detectors. The three dimensional sample position information was fed to a computer that generated and sent appropriate x , y , and z position control signals to high voltage amplifiers so that a prefixed sample position can be maintained. The lower electrode was surrounded by four coils that generated a rotating magnetic field that was used for rotation control⁷⁾. Specimens were prepared by arc melting into spheroids with diameters of around 2 mm. The purity of each element is listed in Table-1.

Three laser beams were used for sample heating (Fig. 1). The beam of one CO₂ laser (10.6 μm emission) was sent directly to the sample whereas that from another CO₂ laser was divided into two beams such that the three focused beams in a same plane, separated by 120 degrees, hit the specimen. This configuration provided temperature homogeneity, improved sample position stability, and helped to control sample rotation.

The radiance temperature was measured with a single-color pyrometer (0.90 μm , 120 Hz acquisition rate) covering a 900 to 3800 K interval. The temperature was calibrated to true temperature using the melting plateau of the sample ($T_m = 1191$ K for La, 1204 K for Pr, 1294 K for Nd, and 1629 K for Tb).

The sample was observed by three charge-coupled-device (CCD) cameras. One color camera offered a view of both the electrodes and the sample whereas two black and white high-resolution cameras (camera-1 and camera-2), located at right angles from each other and equipped with telephoto objectives, provided magnified views of the sample for density measurements. This also helped to monitor the sample position in the horizontal plane and to align the heating laser beams to minimize photon-induced horizontal sample motion and sample rotation⁸⁾.

Table-1 Information of rare earth samples used in electrostatic levitation experiments

	Purity (mass %)	Shape	Manufacturer
La	99.9	Rod	Nilaco
Pr	99.9	Rod	Nilaco
Nd	99.9	Rod	Nilaco
Tb	99.9	Foil	Nilaco

2.2. Thermophysical Property Determination

Density measurements were carried out using a UV imaging technique described in detail elsewhere^{4,9)}. First, a solid sample was levitated and rotation about the vertical-axis was induced by a rotating magnetic field. The rotation rate of the solid sample was measured by a rotation detector, which monitored the intensity of He-Ne lasers reflected from the uneven sample surface⁷⁾. When the rotation rate reached 10 Hz, the rotating magnetic field was turned off. All CO₂ laser beams were directed in such a way to minimize photon-induced rotation during the sample heating. Once a levitated sample was melted, it became spherical due to surface tension and the distribution of surface charge. If the shape of a molten sample departed from that of a sphere (due to excessive rotation), a counter torque was applied by the magnetic field to restore the spherical shape. The controlled sample rotation not only improved the temperature homogeneity of the sample, but also prevented precession and ensured the axi-symmetry of the sample along the vertical axis.

Images at the rate of 30 frames/s and temperature data were simultaneously recorded as a function of time. All laser beams were then blocked with mechanical shutters allowing the sample to cool radiatively. After the experiment, the video images from one high-resolution camera were digitized. Since the sample was axi-symmetric, the sample volume (V) could

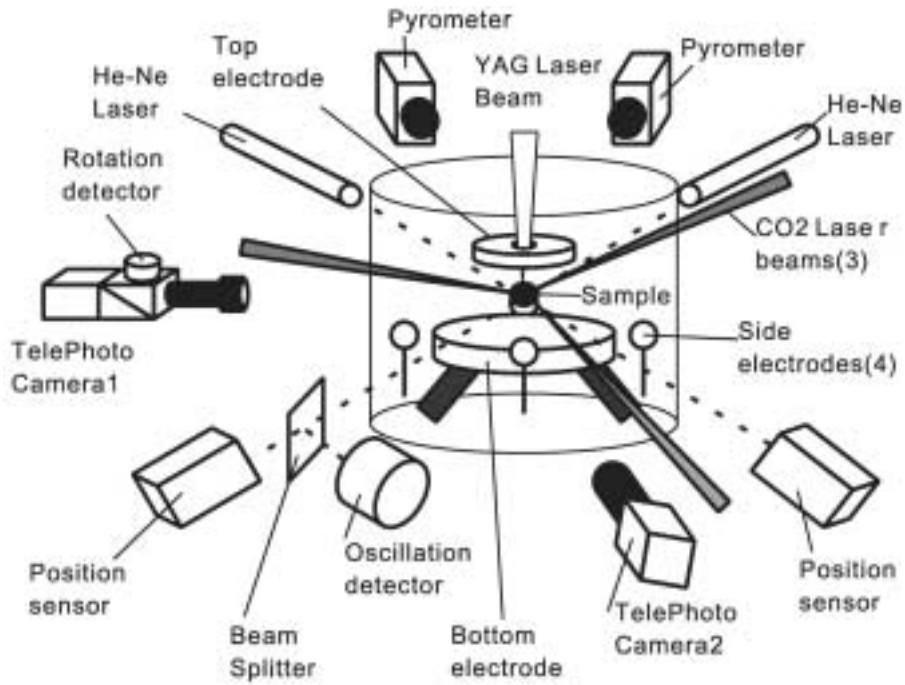


Fig. 1 Schematic view of the electrostatic levitation furnace and its diagnostic apparatus.

be calculated from each image. The recorded images were calibrated by levitating a stainless sphere with a precisely known radius under identical experimental conditions. The images were then matched with the thermal history of the sample (Fig. 2). Because the mass of the sample (m) was known, the density could be determined as a function of temperature with the following equation;

$$\rho = m/V. \quad (1)$$

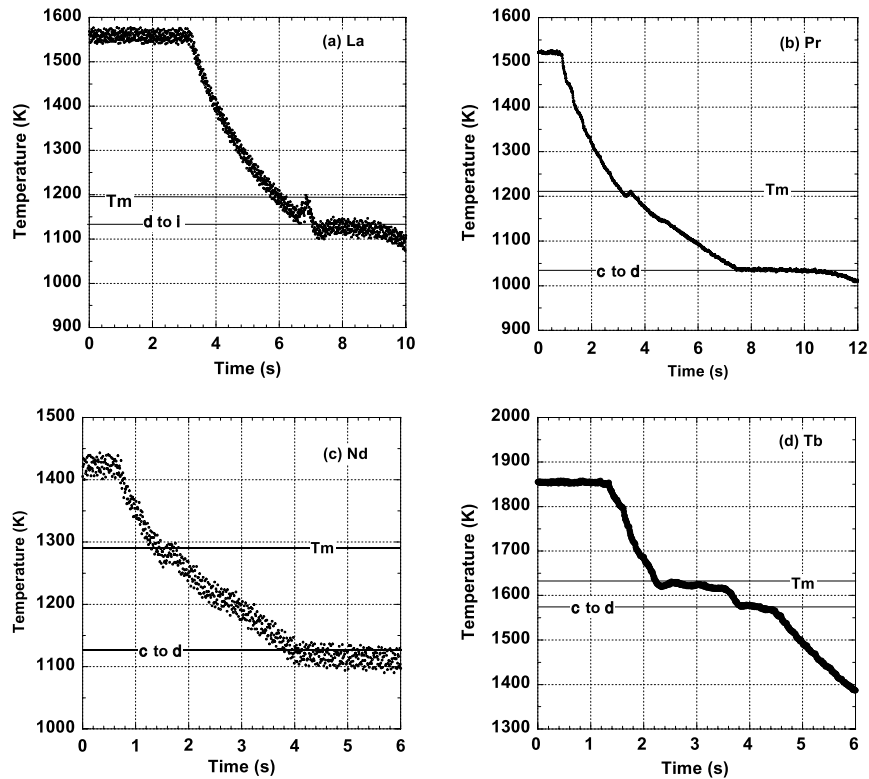


Fig. 2 Radiative temperature profile for molten rare earths samples; (a) La, (b) Pr, (c)Nd, and (d)Tb. All four elements showed solid phase transition after solidification.

Although the sample evaporated as evidenced by a change in radius during long levitation periods (hours), the density experiments lasted only a few minutes, for which the melting temperature was exceeded for only a few seconds (Fig. 2). Therefore, the effect on density was negligible.

The surface tension and viscosity were determined by the oscillating drop method¹⁰. In this method, a solid sample was first levitated, rotated around 10 Hz, heated, melted, and brought to a selected temperature. Then, a $P_2(\cos\theta)$ -mode drop oscillation was induced to the sample by superimposing a small sinusoidal electric field on the levitation field. One of the positioning He-Ne laser beams was divided by a beam splitter and lead to an oscillation detector, which consisted of a power detector and a vertical slit. The shadow of the levitated sample was projected on this detector and variation of the vertical diameter of the sample was translated to an electrical signal. The transient signal that followed the termination of the excitation field was detected and analyzed using a custom-made program. This was done several times at a given temperature and repeated for several temperatures. Using the characteristic oscillation frequency ω_c of the signal, which was calculated by a fast Fourier transform (FFT) analysis and then corrected for non uniform surface charge distribution, the surface tension γ can be determined from¹¹:

$$\omega_c^2 = \left(\frac{8\gamma}{\rho r_0^3} \right) Y, \quad (2)$$

where r_0 is the radius of the sample, ρ is the density, and Y is the correction factor that depends on the drop charge, the permittivity of vacuum, and the applied electric field^{12, 13}. Similarly, using the decay time τ given by the same signal, the viscosity η can be determined by

$$\eta = \frac{\rho r_0^2}{5\tau}. \quad (3)$$

During the experiments, the video images from a high-resolution camera were recorded. After the experiment, each value of the radius at each oscillation was obtained by image analysis. This procedure eliminated the measurement error due to sample evaporation. Moreover, the aspect ratio of the sample (ratio between the horizontal and vertical radii) was also calculated to evaluate the experimental error induced by sample rotation.

2.3. Experimental Uncertainties

The experimental uncertainty for density measurements was derived from the respective uncertainty measurements for the mass and volume of samples. Because the uncertainty in mass was 0.1 mg while a typical sample mass was around 30 mg, the uncertainty can be estimated to be around 0.3 %. The uncertainty of volume ($\Delta V/V$) can be calculated by

$$\frac{\Delta V}{V} = \frac{3\Delta r_0}{r_0} \quad (4)$$

where Δr_0 is the uncertainty in radius measurement by the image analysis⁹. In our experiment, the average value of Δr_0 was around 1 pixel, while r_0 was 160 pixels. Therefore, $\Delta V/V$ can be estimated to be around 1.9 %, and the overall uncertainty of density measurement ($\Delta\rho/\rho$) was estimated to be about 2 %.

Based on equation (2), the uncertainty in surface tension measurement was mainly determined by those of ρ , r_0 , and ω_c . As described earlier, the uncertainty of ρ and r_0 were 2 % and 0.65 %, respectively. The uncertainty of ω_c induced by the FFT analysis was negligibly small (0.4 %) and evaluated by considering the transformation error (less than 1 Hz) and the typical characteristic oscillation frequency (around 250 Hz). As a result, the uncertainty of surface tension measurements ($\Delta\gamma/\gamma$) can be estimated to be around 3 % by the following equation:

$$\frac{\Delta\gamma}{\gamma} \approx \sqrt{\left(\frac{\Delta\rho}{\rho} \right)^2 + \left(\frac{3\Delta r_0}{r_0} \right)^2 + \left(\frac{\Delta\omega_c}{\omega_c} \right)^2}. \quad (5)$$

Similarly, the uncertainty of viscosity measurement can be estimated by the uncertainties of ρ , r_0 , and τ . The

uncertainty of the decay time $\Delta\tau$ was estimated to be about 15 %, which was due mainly to the sample motion with respect to the detector during drop oscillation. This determined the overall uncertainty of viscosity.

3. Results and Discussions

3.1. Density

As shown in figures 2, upon closing the shutters of all heating lasers, each La, Pr, Nd, and Tb samples exhibited slight undercooling, liquid-solid transition, as well as the allotropic transitions (La: fcc to bcc, 1134 K; Pr: Nd: cph to bcc, 1128 K)¹⁵. The density measurements of liquid lanthanum, praseodymium, neodymium, and terbium are shown in Fig. 3.

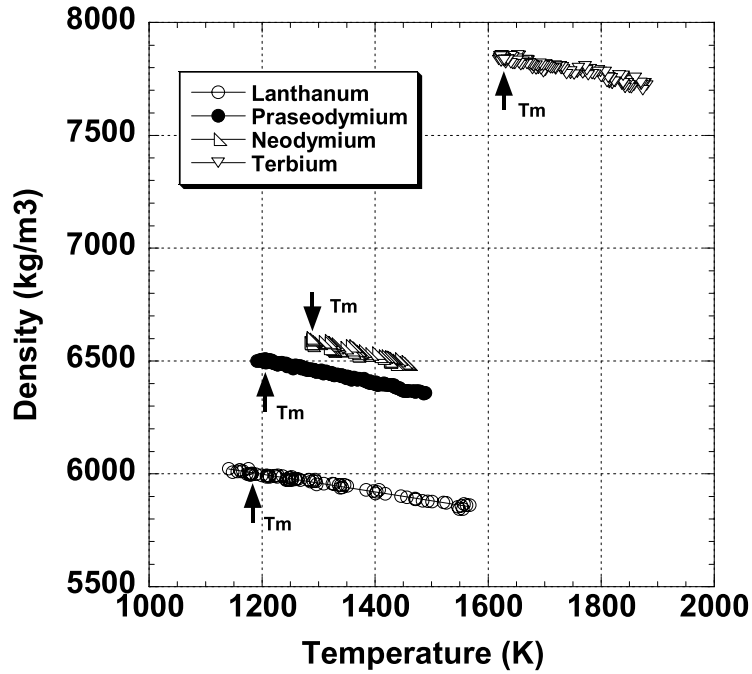


Fig. 3 Density of liquid rare earths versus temperature

Each density data, like that of other pure metals, exhibits a linear behavior as a function of temperature. The measured data and reference values are listed in Table-2. The volume expansion coefficients at the melting temperature (β_m) are calculated with the following formula;

$$\beta = -\frac{1}{\rho} \cdot \frac{d\rho}{dT} \quad (6)$$

A simple relationship between the temperature dependence of the density of liquid metals and their boiling temperatures (T_b) was proposed by Steinberg²¹. He collected liquid density data at the melting point and the temperature dependence of liquid density for 44 elements and found the following empirical relations

$$-\frac{d\rho}{dT} \propto \frac{\rho_{00}}{T_b} \quad (7)$$

where ρ_{00} was the virtual density of the liquid at 0 K determined by extrapolation from ρ_m and T_m with:

$$\rho_{00} = \rho_m - \frac{d\rho}{dT} T_m \quad (8)$$

Figure 4 illustrates the correlation of $-d\rho/dT$ with ρ_{00}/T_b . In this study, most of metal elements followed the correlation. In Fig.4, our measured data of refractory metals²²⁻²⁶ and those of rare earth elements were also plotted. Our data of rare earths, as well as those for other refractory metals, showed a good agreement with Steinberg's relation.

Table-2 Literature Values of the density for liquid rare earths

	$\rho(T_m)$ (kgm^{-3})	$d\rho/dT$ ($\text{kgm}^{-3}\text{K}^{-1}$)	Temperature Range (K)	Volume expansion coefficient $\beta(T_m)$ (10^{-5}K^{-1})	Reference
La	6001 ± 16	-0.39 ± 0.01	1140-1570	6.4	Present work
	5957	-0.237	1224-1277	3.9	Wittenberg ¹⁶⁾
	5955	-0.242		4.1	Wittenberg ¹⁾
	5940	-0.61	1191-1873	10.3	Kononenko ¹⁷⁾
Pr	6500 ± 9	-0.51 ± 0.01	1190-1490	7.8	Present work
	6611	-0.24	1210-1278	3.6	Wittenberg ¹⁶⁾ , Eichelberger ¹⁸⁾
	6500	-0.93	1204-1730	14.3	Kononenko ¹⁷⁾
Nd	6585 ± 55	-0.57 ± 0.04	1280-1460	8.7	Present work
	6890	-0.76	1294-1630	11.3	Kononenko ¹⁷⁾
	6688	-0.528	1294-1520	7.9	Rohr ¹⁹⁾
Tb	7839 ± 39	-0.47 ± 0.02	1615-1880	6.1	Present work
	7679	-0.48	1629-1780	6.3	Stankus ²⁰⁾
	8050	-1.39	1629-1780	17.3	Kononenko ¹⁷⁾

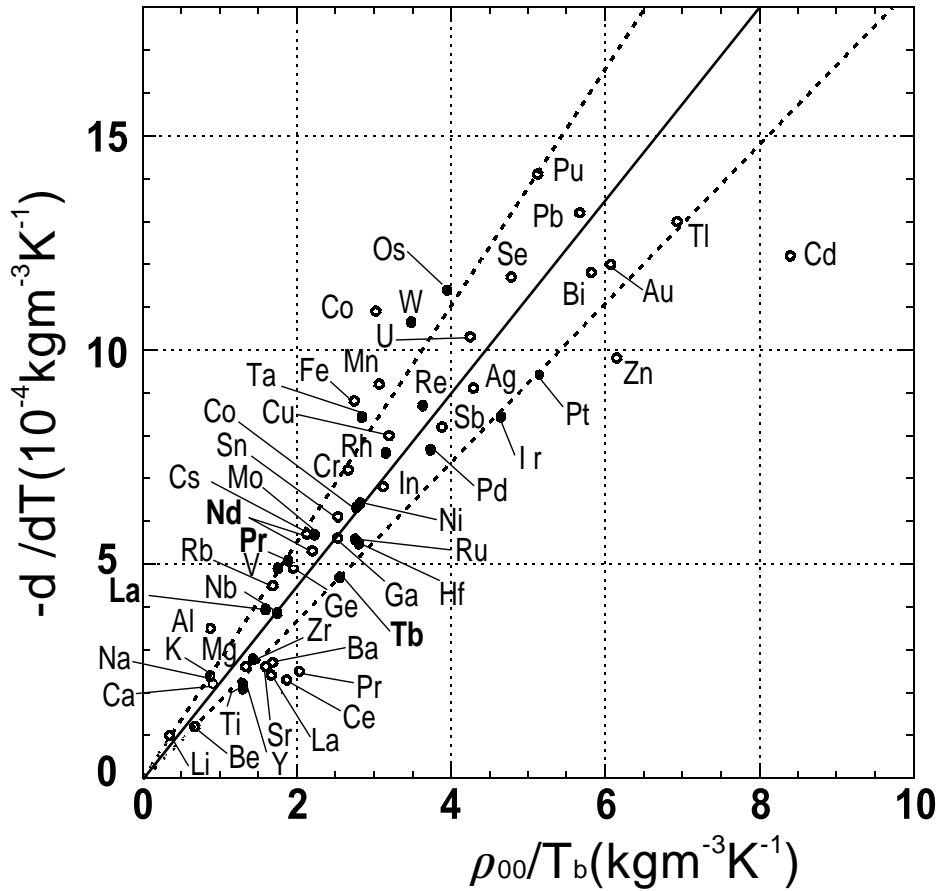


Fig. 4 Correlation of $d\rho/dT$ with ρ_{00}/T_b for elements. Open and black circles represent data from Ref.21 and data measured by an electrostatic levitator, respectively. The solid line is the best fit to the data and the dashed lines represent the 20% error cone from Ref.21.

3.2. Surface Tension

Figure 5 depicts the results for the surface tension of rare earths as a function of temperature. Like the density data, the surface tension data show a linear temperature dependence. Table-3 summarizes our measurement data and reference values. Because rare earth elements are very easily oxidized, surface tension measurements in the undercooled region were very hard to perform. Improvement of vacuum level is necessary to get data in this region.

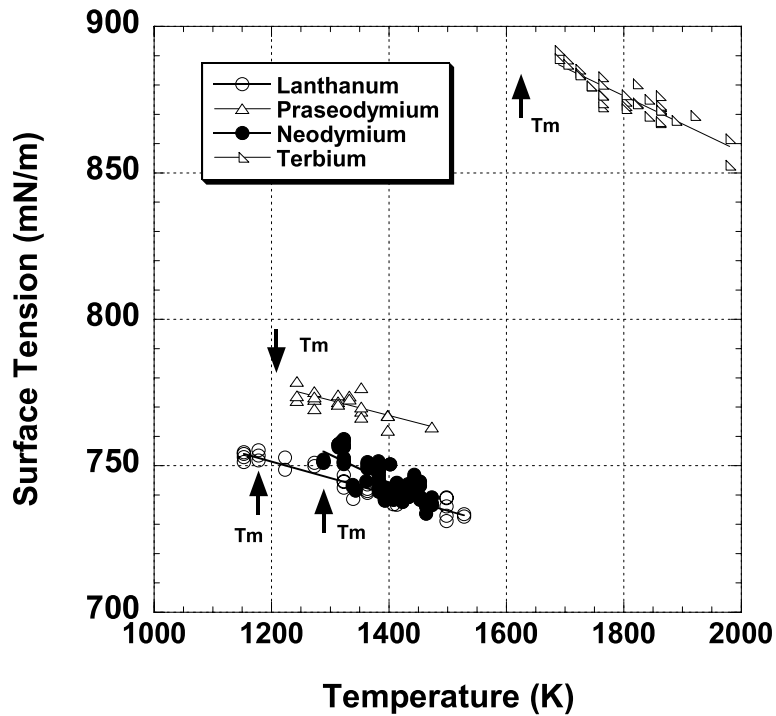


Fig. 5 Surface tension of rare earths versus temperature.

When considering the experimental uncertainties, our results at the melting temperature show excellent agreement with the works of Chentsov²⁷⁾ and Bezukladnikova et al.²⁸⁾ (La) and those of Bezukladnikova et al.²⁸⁾ (Pr). For Nd and Tb, our results were systematically higher than the literature data. The lower surface tension data reported elsewhere could be explained by the fact that the measurements were done with techniques for which a contact between a molten sample and a surface (e.g., sessile drop technique) occurred, which is not the case with our technique. The contact could have further contaminated the surface of the sample and therefore lowered the surface tension³⁶⁾. Additional surface contamination could have occurred for samples that were processed under non-high vacuum conditions because of the oxygen and nitrogen affinity of those rare earths¹⁾.

Table-3 Literature values of the surface tension for liquid rare earths

	$\gamma(T_m)$ (10^{-3}Nm^{-1})	$d\gamma/dT$ ($10^{-3}\text{Nm}^{-1}\text{K}^{-1}$)	Temperature Range (K)	Reference
La	752 ± 9	-0.056 ± 0.007	1150-1525	Present work
	745	-0.10	1191-1650	Chentsov ²⁷⁾
	739	-0.106	1191-1620	Bezukladnikova ²⁸⁾
	729	-0.098	1191-1750	Sukhman ²⁹⁾
	728	-0.10	1191-1873	Kononenko ¹⁷⁾
	701		1191	Martsenyuk ³⁰⁾
	700		1191	Kingery ³¹⁾
	720	-0.32		Pulliam ³²⁾
Pr	777 ± 29	-0.052 ± 0.02	1240-1475	Present work
	690	-0.073	1204-1730	Kononenko ¹⁷⁾
	690	-0.071	1204-1800	Sukhman ²⁹⁾
	723		1204	Martsenyuk ³⁰⁾
	743	-0.092	1204-1873	Bezukladnikova ²⁸⁾
Nd	754 ± 25	-0.095 ± 0.018	1290-1475	Present work
	685	-0.07	1289-1630	Kononenko ¹⁷⁾
	685	-0.087	1289-1630	Sukhman ²⁹⁾
	688		1294	Lasarev ³³⁾
	689	-0.09		Lasarev ³⁴⁾
Tb	823 ± 28	-0.096 ± 0.015	1690-1980	Present work
	700		1629	Fogel ³⁵⁾
	669	-0.056	1629-1780	Sukhman ²⁹⁾

It is well known that the surface tension at melting temperature (γ_m) shows a good correlation with the following function^{17,37)}:

$$\gamma_m \propto \frac{RT_m}{V_m^{2/3}} \quad (9)$$

where R is the gas constant ($8.31 \text{ J}\cdot\text{mol}^{-1}\cdot\text{K}^{-1}$), and V_m is the molar volume at the melting temperature. Fig.6 depicts the correlation between γ_m and $(RT_m(V_m)^{-2/3})$ for 57 metal elements. Our measurement data of La, Pr, Nd, and Tb as well as other refractory metals showed a good agreements with equation (9).

Compared with refractory metals, temperature coefficients of rare earths are small (less than $-0.1 \text{ mNm}^{-1}\text{K}^{-1}$). The literature values for Nd and La agree with our data. However, our data for Pr and Tb were respectively around 50% smaller and 70% higher than that of literature values. Kasama *et al.*³⁸⁾ proposed an empirical equation based on a physical model. Based on this model, surface tension and its temperature dependence can be expressed as

$$\gamma = \frac{1}{2} \frac{\pi^2 C^2 \delta^2 T_m}{N_A M^{2/3}} \left(\frac{\rho}{\rho_m} \right)^{2/3} \{ (\alpha + 1) \rho^{1/3} - \rho_m^{1/3} \}^2$$

$$\frac{d\gamma}{dT} = -\frac{1}{3} \frac{\pi^2 C^2 T_m \Lambda \delta^2}{N_A M^{2/3}} \{ 2(\alpha + 1)^2 \rho^{1/3} \rho_m^{2/3} + \rho^{-1/3} - 3(1 + \alpha) \rho_m^{-1/3} \} \quad (10)$$

where N_A was Avogadro's number, M was the atomic number, Λ was the temperature dependence of density ($-dp/dT$), C was a constant derived from Lindemann's theory of melting (ranged from 2.8×10^{12} to 3.1×10^{12}), δ was the ratio between the characteristic vibration frequency in the liquid phase and the solid phase (estimated to be around 0.5), and a was a

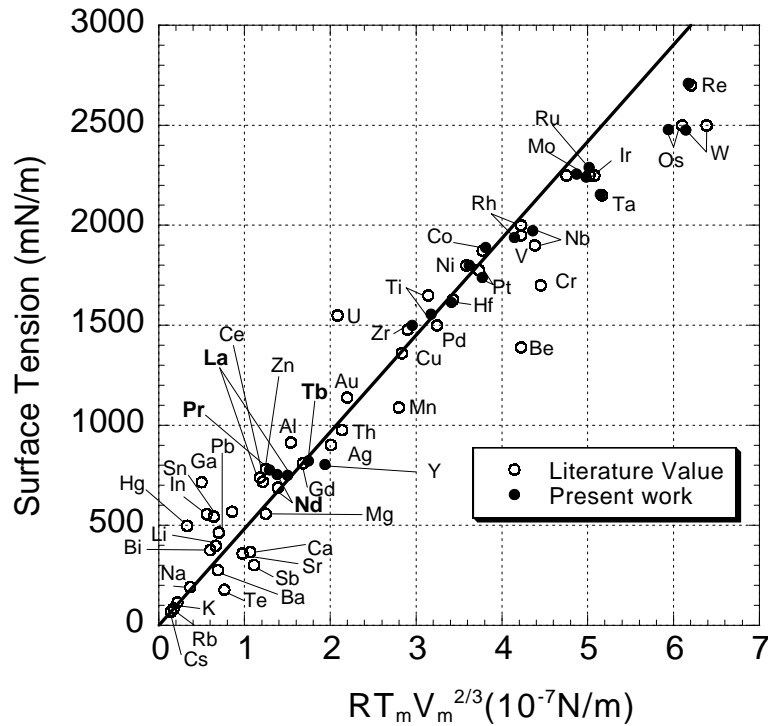


Fig. 6 Correlation of surface tension γ_m with $(RT_m/V_m^{2/3})$ for various liquid metals.

constant indicating the distance where an attractive force by an atom was effective (ranged from 0.45 to 0.65).

At the melting temperature, the temperature coefficient of the surface tension could be calculated by

$$\frac{d\gamma}{dT} = -\frac{1}{3} \frac{\pi^2 C^2}{N_A} \frac{T_m \Lambda \delta^2}{M^{2/3}} \rho_m^{-1/3} (2\alpha^2 + \alpha) \quad (11)$$

In this formula, the uncertainties of the constants (C , a , and δ) seriously affected the temperature dependence of the surface tension. Two of those constants could be eliminated by combining equations (10) and (11), and the temperature coefficient of the surface tension could be determined as

$$\begin{aligned} \frac{d\gamma}{dT} &= -\frac{2}{3} \frac{\Lambda \gamma_m}{\rho_m} \frac{2\alpha + 1}{\alpha} = K \frac{\Lambda \gamma_m}{\rho_m} = K \gamma_m \beta_m \\ K &\equiv \frac{-2(2\alpha + 1)}{3\alpha} \end{aligned} \quad (12)$$

This equation suggested that the temperature dependence of the surface tension was proportional to the product of the surface tension at the melting temperature and the thermal expansion coefficient.

Validity of this formula for liquid metals was checked by using literature data³⁹⁻⁴¹⁾ and our measurements obtained with the electrostatic levitator (ESL)⁴²⁻⁴⁴⁾. Results are shown in figure 7.

Literature data for alkaline metals showed good agreements with equation (12), while those for transition metals exhibit scatter, some being far from the relation. Particularly, data for lanthanum is far out of the proposed correlation. On the other hand, measured data of refractory metals with ESL showed the same tendency as the alkaline metals. Based on the ESL results, temperature dependence of surface tension of metal elements could be estimated if the surface tension at the melting temperature and if the thermal expansion coefficient were known.

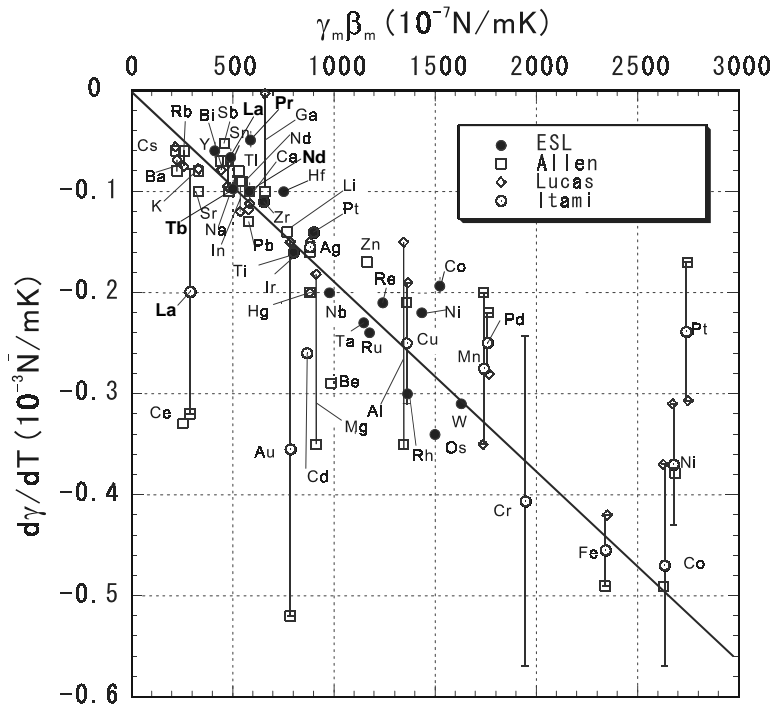


Fig. 7 Correlation between $\gamma_m \beta_m$ and $d\gamma/dT$

3.3. Viscosity

Figure 8 illustrates our viscosity data that can be fitted by the following Arrhenius function:

$$\eta(T) = \eta_0 \exp(E/RT) \tag{13}$$

where R is the gas constant ($8.31 \text{ J}\cdot\text{mol}^{-1}\cdot\text{K}^{-1}$), η_0 is the pre-exponential viscosity, and E is the activation energy. Values of η_0 and E are listed in Table-4 together with literature values. The scatter observed in the data is mainly due to the motion of the sample with respect to the oscillation detector. No other experimental values were found for Nd and Tb.

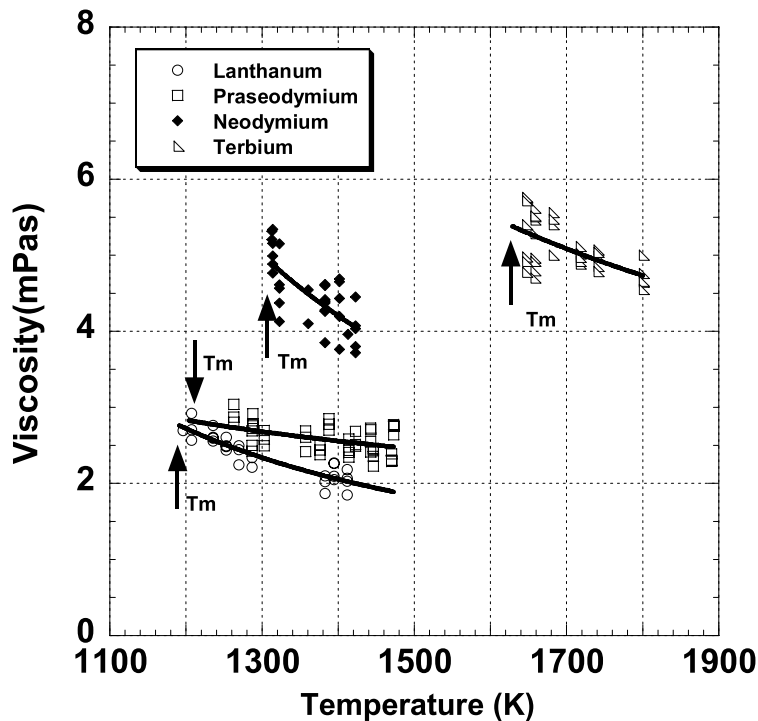


Fig. 8 Viscosity of rare earth metals versus temperature.

Table-4 Literature values of the viscosity for liquid rare earths

	$\eta(T_m)$ (mPa·s)	$\eta(T)=\eta_0\exp(E/RT)$		Temperature Range (K)	Reference
		η_0 (mPa·s)	E (kJ·mol ⁻¹)		
La	2.75	0.381	19.6	1195-1410	Present work
	2.45	0.209	25.2	1191	Wittenberg ⁴⁵⁾
	3.13	0.2317	26.255	1213-1493	Frohberg ⁴⁶⁾
	2.65				Iida ³⁷⁾
Pr	2.82	1.38	7.14	1260-1475	Present work
	2.80	0.936	11.2	1204-1280	Wittenberg ⁴⁵⁾
	2.80	1.758	4.678		Lucas ⁴⁰⁾
	2.85				Iida ³⁷⁾
Nd	5.07	0.43	26.5	1310-1420	Present work
Tb	5.3	1.399	18.2	1647-1800	Present work

The most successful quantitative correlation between the viscosity of liquid metal and other thermophysical properties is that of Andrade^{47,48)}. Andrade obtained the following formula by assuming that the characteristic vibration frequency in the liquid at the melting point is equal to that in the solid, which can be estimated from the Lindemann's law⁴⁹⁾;

$$\eta(T_m) = CA \sqrt{\frac{MT_m}{V_m^{2/3}}} \quad (14)$$

where M is the atomic mass. Fig.9 illustrates the validity of the Andrade's formula with the measured data by ESL and other literature data. Except for Nd, the viscosity of rare earth metals shows good agreement with the formula. The current uncertainty of viscosity measurement is around 20% or more. Improvement of viscosity measurement is necessary to quantitatively evaluate the validity of Andrade's formula.

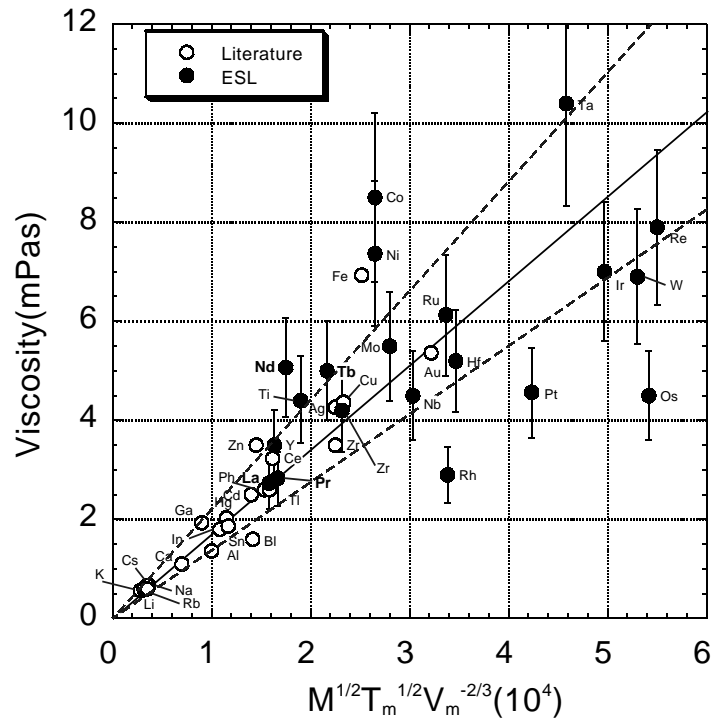


Fig. 9 Correlation between $M^{1/2} T_m^{1/2} V_m^{-2/3}$ and viscosity based on Andrade's formula. Measured values by ESL (black circle) are shown with 20% error bar.

4. Conclusions

The density, the surface tension, and the viscosity of four rare earth metals were measured with an electrostatic levitator. The containerless processing and non-contact measurement techniques eliminated contamination from the crucibles as well as suppressed nucleation at the melting temperature. This enabled the measurement of the thermophysical properties over wide temperature ranges. The measured data of rare earth metals, coupled with other refractory metals' data, were compared with literature values as well as estimated data based on several correlation formulae.

Acknowledgments

This work was supported by a Grant-in-Aid for Scientific Research (B) from the Japan Society for the Promotion of Science.

REFERENCES

1. D. R. Lide and H. P. R. Frederikse: *CRC Handbook of Chemistry and Physics*, (CRC Press, Boca Raton, Florida, 1997) 78th ed.
2. P.-F. Paradis, T. Ishikawa, and S. Yoda: *ESA SP-454* (2001), 993.
3. T. Ishikawa, P.-F. Paradis, and S. Yoda, *J. Jpn. Soc. Microg. Appl.* **18** (2001), 106.
4. T. Ishikawa, P.-F. Paradis, and S. Yoda: *Rev. Sci. Instrum.* **72** (2001), 2490.
5. P.-F. Paradis, T., Ishikawa, and S. Yoda, *Int. J. Thermophys.*, **23**, (2002), 825.
6. W.-K. Rhim, S.-K. Chung, D. Barber, K.-F. Man, G. Gutt, A. A. Rulison, and R. E. Spjut, *Rev. Sci. Instrum.* **64** (1993) 2961.
7. W.-K. Rhim and T. Ishikawa, *Rev. Sci. Instrum.* **69** (1998) 3628.
8. W.-K. Rhim and P.-F. Paradis, *Rev. Sci. Instrum.* **70** (1999) 4652.
9. S.-K. Chung, D. B. Thiessen, and W.-K. Rhim, *Rev. Sci. Instrum.* **67** (1996) 3175.
10. W.-K. Rhim, K. Ohsaka, P.-F. Paradis, and R. E. Spjut, *Rev. Sci. Instrum.* **70** (1999), 2996.
11. Lord Rayleigh, *Proc. R. Soc. London* **29** (1879), 71.
12. Lord Rayleigh, *Philos. Mag.* **14** (1882), 184.
13. J. Q. Feng and K. V. Beard, *Proc. R. Soc. London A* **430** (1990), 133.
14. H. Lamb, *Hydrodynamics* (Cambridge University Press, 1932) 6th ed., 473.
15. A. T. Dinsdale, *CALPHAD*, **15**, (1991), 317.
16. L. J. Wittenberg, D. Ofte, and W.G. Rohr, "Rare Earth Research", Vol II ed. K.S. Vorres, Gordon and Breach, (1964), 257.
17. V. I. Kononenko, A. L. Sukhman, S. L. Gruverman, and V. V. Torokin, *Phys. Stat. Solid.*, **84A**, (1983), 423.
18. J. F. Eichelberger, Mound Lab. Rep. 1118, (1961), 12.
19. W. G. Rohr, *J. Less Common Metals*, **10**, (1966), 389.
20. S. V. Stankus, A. S. Basin, Tezisi. VII vsesoyuznoi konf. Teplofizicheskie svoistvaveschestv, chap.2, Inst. Teplofiz. Sov., AN SSSR (in Russian), Novosibirsk (1982), 80.
21. D. J. Steinberg, *Metallurgical Transactions* **5** (1974), 1341.
22. T. Ishikawa, P.-F. Paradis, T. Itami, and S. Yoda, *Meas.Sci. Technol.* **16** (2005), 443.
23. T. Ishikawa and P.-F. Paradis, *Journal of Electronic Materials*, **34** (2005), 1526.
24. P.-F. Paradis, T. Ishikawa, R. Fujii, and S. Yoda, *Appl. Phys. Lett.* **86** (2005), 41901.
25. T. Ishikawa, P.-F. Paradis, and N. Koike, *JJAP* **45** (2006), 1719.
26. P.-F. Paradis, T. Ishikawa, and N. Koike, *JAP* **100** (2006), 103523.

27. V. P. Chentsov, Dissertation Inst. Tekh. Metallurgiya UNTs, Akad. Nauk. SSSR, Sverdlovsk, 1972.
28. L. L. Bezukladnikova, V. I. Kononenko, V.V. Torokin, *Teplofiz. Vys. Temp.*, **27**, (1989), 478.
29. A. L. Sukhman, V. I. Kononenko, S. L. Gruverman, and V. V. Torokiv, *Poverkhnostnye svoistva rasplavov* (Surface properties of melts) (in Russian), 107, Nauka Dumka, 1982.
30. P. S. Martsenyuk, and Y. N. Ivashchenko, *Adgez. Rasp. Paika Mater.*, **19**, (1984), 12.
31. W. D. Kingery, *Amer. Ceram. Soc. Bull.*, **35**, (1956), 108.
32. G. R. Pulliam, and E. S. Fitzsimmons, Report US Atom. Energy Comm, Ames Lab. Rep. No.ISC-659-1955, 1955.
33. A. Lasarev and I. V. Pershikov, *Doklady A.N.*, **146**, (1962), 143.
34. V. B. Lasarev and A. V. Pershikov, *Proc. Acad. Sci. USSR, Phys. Chem. Sect.* **146**, (1962), 637.
35. A. A. Fogel, T. A. Sidorova, G. E. Chuprikov, M. M. Mezdrogina, *Izv. Akad. Nauk SSSR Metal.*, **1** (1965), 50.
36. B. J. Keene, "Surface Tension of Pure Metals", National Physical Laboratory, Publication DMM(A) 39, 1991.
37. T. Iida and R. I. L. Guthrie: *The Physical Properties of Liquid Metals*, (Clarendon Press, Oxford 1988).
38. A. Kasama, T. Iida, and Z. Morita, *J. Japan Inst. Metals*, **40** (1976), 1030.
39. B. C. Allen, *Trans. AIME* **227** (1963), 1175.
40. L. D. Lucas, *Tech l'Ing.*, **7**, Form. M65 (1984).
41. T. Itami, in *Condensed Matter Disordered Solids*, ed. S. K. Srivastava and N. H. March (World Scientific. 1995), Chap.3
42. T. Ishikawa, P. -F. Paradis, T. Itami, and S. Yoda, *JAXA Research and Development Report*, JAXA-RR-04-024E (2005).
43. T. Ishikawa, P. -F. Paradis, and N. Koike, *JAXA Research and Development Report*, JAXA-RR-05-015E (2006).
44. T. Ishikawa, P. -F. Paradis, and N. Koike, *JAXA Research and Development Report*, JAXA-RR-06-012E (2007).
45. L. J. Wittenberg and R. DeWitt, in *The properties of Liquid Metals*, (ed. by S. Takeuchi), Taylor & Francis, London (1973), 555.
46. M. Frohberg and T. Cakici, *Z. Metallkunde*, **69**, (1978), 296.
47. L. Battezzati and A. L. Greer, *Acta Metall.* **37** (1989), 1791.
48. E. N. Da C. Andrade, *Phil. Mag.* **17** (1934), 497.
49. F. A. Lindemann, *Phys. Z.* **11** (1910), 609.

JAXA Research and Development Report JAXA-RR-07-014E

Date of Issue : February 29, 2008

Edited and Published by : Japan Aerospace Exploration Agency

7-44-1 Jindaiji-higashimachi, Chofu-shi, Tokyo 182-8522, Japan

URL: <http://www.jaxa.jp/>

Printed by : Printoffice ZERO

Inquires about copyright and reproduction should be addressed to the Aerospace Information Archive Center, Information Systems Department JAXA.

2-1-1 Sengen, Tsukuba-shi, Ibaraki 305-8505, Japan

phone: +81-29-868-5000 fax: +81-29-868-2956

Copyright © 2008 by JAXA

All rights reserved. No part of this publication may be reproduced, stored in retrieval system or transmitted, in any form or by any means, electronic, mechanical, photocopying, recording, or otherwise, without permission in writing from the publisher.

